

## Grammatical complexity of strange sets

Ditza Auerbach and Itamar Procaccia

*Department of Chemical Physics, The Weizmann Institute of Science, Rehovot 76100, Israel*

(Received 3 January 1990)

Chaotic dynamical systems can be organized around an underlying strange set, which is comprised of all the unstable periodic orbits. In this paper, we quantify the complexity of such an organization; this complexity addresses the difficulty of predicting the structure of the strange set from low-order data and is independent of the entropy and the algorithmic complexity. We refer to the new measure as the *grammatical complexity*. The notion is introduced, discussed, and illustrated in the context of simple dynamical systems. In addition, the grammatical complexity is generalized to include metric properties arising due to the nonuniform distribution of the invariant measure on the strange set.

### I. INTRODUCTION

An important step in understanding chaotic motion has been the hierarchical resolution of strange attractors around a skeleton furnished by the multitude of unstable periodic orbits. These are dense on hyperbolic strange attractors (those whose tangent space can be continuously decomposed into disjoint stable and unstable manifolds).<sup>1</sup> It is conjectured that this is also the case for generic strange attractors. Moreover, the number of periodic points (in discrete time) belonging to orbits of length  $n$  increases exponentially with  $n$  (according to the topological entropy<sup>2</sup>), rendering it natural to hierarchically construct the strange attractor around the set of periodic points of increasing order. It has been demonstrated in a number of relevant and interesting cases<sup>3-7</sup> that this approach leads to a sensible, convergent scheme for describing strange attractors and their properties. An important characteristic of the periodic orbits and their Lyapunov exponents is their independence of coordinate representation, rendering them relevant quantities to be extracted from data. In fact, a numerical procedure for obtaining the unstable periodic orbits and their Lyapunov exponents from a chaotic time series has been developed.<sup>3</sup>

A real chaotic trajectory can be considered as a random walk in phase space among the unstable cycles; it approaches a periodic orbit along its stable manifold, only to be subsequently thrown away from it along its unstable manifold onto the stable manifold of another periodic orbit. The difficulty in characterizing the set of allowed periodic orbits to arbitrary length and the transitions between them is equivalent to the effort necessary to reconstruct the chaotic trajectories of the system. The naive notion of a simple system is one in which low-order data, i.e., only information on the short periodic orbits, is sufficient in order to predict the properties of periodic orbits of arbitrarily long length. For a nonsimple or complex system, finite data are insufficient in order to characterize all the properties of arbitrarily long orbits correctly. It is this intuitive notion of complexity that will be quantified in the following.

When the dynamical system has a good symbolic dy-

namics, the characterization via the strange set of periodic orbits is particularly useful. One can generate a language with every allowed periodic point identified by a word in this language. One is interested in determining the *rules* that specify which words are allowed and which are missing. If a finite number of rules enables the prediction of all the allowed words of arbitrary length, we shall say that the dynamical system is grammatically trivial. On the other hand, if the number of rules needed to predict which orbits are allowed increases with orbit length, then we shall call the dynamical system grammatically complex. In this paper, we consider only systems whose dynamics can be represented by symbolic sequences of a finite alphabet. It should be stressed that there is no relation between the grammatical complexity and entropylike quantities such as the Kolmogorov complexity.<sup>8,9</sup> Entropylike quantities are employed to measure the degree of unpredictability or randomness, rather than to provide an indication of the difficulty with which the set of all possible motions can be organized and encoded. For example, in the family of unimodal maps, the parameter value corresponding to the case of fully developed chaos has the maximal Kolmogorov-Sinai entropy of  $\ln 2$ . On the other hand, using the usual binary dynamics of 0 and 1, one sees that the system is grammatically trivial. The rule for the language is that there are no rules; all words (strings of 0's and 1's) are allowed, meaning that the number of periodic points belonging to orbits of length  $n$  increases as  $2^n$ . As will be shown in Sec. III, there are parameter values of unimodal maps with a smaller Kolmogorov-Sinai entropy, whose grammar is nontrivial.

The structure of the paper is as follows. In Sec. II we introduce and quantify the concept of *grammatical complexity* by measuring the difficulty in organizing the periodic orbits on finitely branched complete trees. Other proposed topological definitions of complexity are examined and compared. Calculations of the grammatical complexity is illustrated in Sec. III for several parameter values of the one-dimensional (1D) quadratic map. A generalization of the notion of grammatical complexity, which incorporates the invariant measure on the set in

addition to its topological characteristics, is presented in Sec. IV. The hierarchical convergence of these generalized complexities is discussed in terms of the correlations present in a chaotic trajectory between the basic *building blocks* (indecomposable concatenations of the alphabet symbols that are introduced in Sec. II). Finally, in Sec. V we summarize and address further applications of the new concepts introduced.

## II. GRAMMATICAL COMPLEXITY

Consider a system whose symbolic dynamics is composed of  $k$  symbols, with all its periodic orbits organized on the branches of a complete  $k$ -branch tree. A typical branch splits into  $k$  daughters, each being a concatenation of the mother orbit with one of the  $k$  basic symbols (see Fig. 1). All the periodic points of length  $n$  are displayed on the  $n$ th level of the tree whose first few levels are shown in Fig. 1. If there are no grammatical rules prescribing the pruning of periodic orbits in the tree hierarchy, the grammar of the system is simple; the presence of all high-order periodic orbits can be deduced solely from the existence of the  $k$  fixed points. On the other hand, its topological entropy is maximal among all grammars composed of  $k$  symbols. For systems with periodic orbits missing, it may still be possible to arrange the allowed periodic orbits on a finitely branched complete tree, whose top level no longer consists of the  $k$  basic symbols; instead, it consists of  $n$  *building blocks*  $\{b_1, b_2, \dots, b_n\}$ , each of which is constructed from concatenations of the  $k$  alphabet symbols. Such a finitely branched tree may faithfully represent only those cycles in a chaotic system which are less than some maximum length.

A system for which the entire set of periodic orbits can be organized on a complete tree with a finite number of building blocks on the top level is defined to have zero grammatical complexity. These building blocks need not necessarily be single orbits but rather families of periodic orbits described by regular expressions<sup>10</sup> composed of concatenations of the basic alphabetic symbols along with the operations  $+$  (exclusive or) and  $*$  (arbitrary repetitions). Also, we require that a block which is reducible to a sum of two blocks (using exclusive or) should be considered as two separate building blocks, so that a single building block represents an indecomposable unit. In the same way that the irrationality of a real number is measured by the difficulty in approximating it by rational numbers, the grammatical complexity quantifies the difficulty in approximating the set of allowed periodic or-

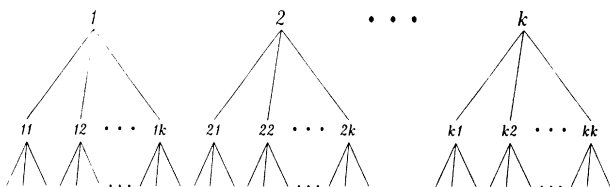


FIG. 1. Structure of a complete  $k$  branch tree of periodic orbits with the  $k$  fixed points on the top level of the tree.

bits by these complete trees of regular expressions. The complete tree approximants to the structure of the set of periodic orbits at the parameter value of interest provide an exact description up to a finite period  $l$  of orbits. Beyond length  $l$ , higher branched complete trees are necessary for an exact description. The grammatical complexity  $C_0$  is defined as the asymptotic growth rate of all the number of building blocks  $n(l)$  necessary for an exact specification of all the cycles up to length  $l$ ,

$$C_0 = \lim_{l \rightarrow \infty} \frac{n(l)}{l} . \quad (1)$$

The lim in the above expression is replaced by lim sup for the cases where the limit does not exist. Zero complexity grammars are those described either by a finite number of building blocks or those that exhibit a slower than linear growth rate of the number of building blocks. Using the results of Appendix A, it is clear that the growth rate cannot be larger than linear and, furthermore, that  $C_0$  has an upper bound of 2 for the case of binary dynamics.

We first outline the procedure for constructing the complete tree approximations for a generic grammar of a parametrized family of dynamical systems. The strategy is to seek nearby parameter values possessing complete tree grammars with a finite number of building blocks. One possibility, and the one we mainly consider, is that these approximating grammars arise due to the presence of a Markov partition of the phase space, defined as one in which each partition element is mapped exactly onto a union of other elements, under the action of the dynamics. Narrowing in on a generic parameter value along Markov partition parameter values usually involves a succession of increasingly finer partitions; in the same way as a sequence of rationals approaching an irrational have increasingly large denominators. At a parameter value corresponding to a Markov partition of  $N$  elements, a directed graph of  $N$  nodes (each denoting a partition element) can be used to represent the topological structure of the dynamics. Directed links emanate from each node to the nodes denoting its preimages. For binary symbolic dynamics, there are at most two links leaving a node, each labeled by either 0 or 1, depending on in which of the two regions of the generating partition the preimage lies. Such graphs represent regular languages and are usually referred to as finite automata.

A periodic orbit can be immediately read off a graph as a path which starts at a given node, traverses directed links, and finally returns to the initial node after a finite number of steps. Although the graph is finite, orbits of arbitrarily long periods may be formed, provided there are closed loops in the graph. Since the graph represents the grammar of an invariant set, there are no transient parts to the graph, i.e., each node is accessible in a finite number of steps from an arbitrary start node. All the periodic orbits beginning at a node  $B$  can be organized on a complete tree whose building blocks  $\{b_1, b_2, \dots, b_n\}$  are the *smallest* set of regular expressions consisting solely of the periodic orbits which begin at  $B$  and return to  $B$  only at the end of their traversal path. All the periodic orbits originating at  $B$  can then be expressed as the regular expression

$$(b_1 + b_2 + \dots + b_n)^*$$

Using this outline, the conversion of a finite directed graph to a complete tree of regular expressions of periodic orbits can always be accomplished. The number of building blocks necessary may vary depending on the starting node chosen, and therefore we now introduce a weighting of the building blocks.

Depending on the node of a graph chosen for a complete tree construction, the building blocks themselves may include the operator “+”. Such a block, say  $b_i = \alpha(\beta + \gamma)^* \delta$ , where  $\alpha, \beta, \gamma, \delta$  denote particular concatenations of 0's and 1's, includes in its definition a complete binary tree composed of all possible combinations of  $\beta$  and  $\gamma$ . This additional branching within the complete tree of building blocks is taken into account in the grammatical complexity by weighting each building block in definition (1) according to the number of secondary branchings it possesses (or equivalently the number of “+” operators it includes). If the identical subtree structure appears in more than one building block, it is not recounted. As will be made clear in the examples, this weight guarantees that the grammatical complexity becomes independent of the starting node used in the finite graph approximants.

In the remainder of this section we comment on the relation of the grammatical complexity to some other existing schemes of analyzing complexity. Grammars that can be represented by a finite number of building blocks belong to the class of regular languages. Generic grammars arising in even the simplest of dynamical systems may not belong to this class, but rather to a higher-level language in the Chomsky hierarchy.<sup>10</sup> Given an exact specification of the allowed strings of a grammar, determining the hierarchy class it belongs to, may be computationally undecidable.<sup>10</sup> In addition to the uncomputability of these grammatical classes, their order in the Chomsky hierarchy does not reflect the degree of difficulty in forecasting detailed features of the grammar from the gross ones, which is the main concern when dealing with dynamical systems. In our approach, a nonregular grammar arising in a dynamical system is considered as a limit of a sequence of regular languages represented by finite graphs whose sizes grow to infinity. In addition to the possibility of explicitly constructing these limiting grammars, the growth rate of the number of building blocks gives a precise measure of the increase in the number of rules necessary for a hierarchical specification of the strange invariant set.

Previously, the framework of regular languages has been used to define the algorithmic complexity.<sup>11</sup> It is given by  $\ln N$  where  $N$  is the number of nodes in the minimum deterministic automaton representing the grammar. This definition for complexity<sup>12,13</sup> typically diverges for generic dynamical systems possessing nonregular grammars. In addition, we argue that the relevant criterion for describing the complexity of a dynamical system is not the number of nodes but rather the number of building blocks. For example, Fig. 2 shows graphs of two systems with different number of nodes whose periodic orbits can be arranged on complete

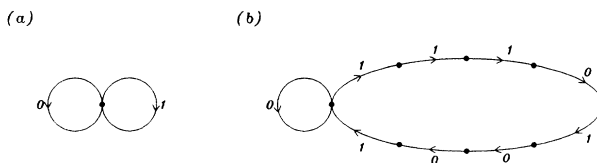


FIG. 2. Graphs of two regular grammars with different number of nodes which can be represented on binary trees. The labeled arrows denote the preimages of a particular node. For case (a) the building blocks are 0 and 1, while for case (b) they are 0 and 10010111. Grammatically they are equally simple.

binary trees. Arbitrarily long periodic orbits can be predicted in both cases from the knowledge of two building blocks; for Fig. 2(a) the building blocks 0 and 1 are sufficient, while for Fig. 2(b) one requires the blocks 0 and 10010111. Although the topological entropy in these two cases differ (due to the different number of nodes), their hierarchical encoding is equally simple.

All previous definitions of complexity which are based on the number of nodes of a finite automaton diverge at points of period-doubling accumulation.<sup>12,13</sup> At these parameter values, the number of periodic points grows slower than exponentially with the length of the period, and thus all the generalized entropies<sup>14</sup> of the system are zero; indeed, the number of periodic orbits grows logarithmically with increasing length of orbits. The hierarchical organization of periodic orbits on a treelike structure implicitly assumes an exponential growth in the multitude of trajectories of increasing length exhibited by the system. In the case of period doubling, such a hierarchy is absent, and in fact the system only exhibits a single trajectory which can be simply specified.<sup>15</sup> The unstable orbits up to length  $l$  can be obtained by simply listing all the  $\ln l$  orbits themselves. According to the limiting procedure of Eq. (1), the grammatical complexity takes on the value zero, which agrees with our intuitive notion of a system possessing a unique trajectory which can be simply reconstructed to arbitrary length.

The most common notion of complexity for symbolic strings involves a quantification of the computational effort necessary to reconstruct the string exactly. The Kolmogorov complexity<sup>8</sup> is given by the size of the minimal numerical procedure that generates the given string on a universal Turing machine. It is in general uncomputable and usually reduces to the information entropy of the string whenever it can be explicitly calculated. Related definitions of computational complexity consider minimal programs running in either bounded space or time.<sup>16</sup> The logical depth,<sup>17</sup> determined by the time required to produce a given string from its minimal program, has also been suggested as a measure of complexity. All the variants of such definitions suffer from the fact that they are in general uncomputable and are concerned with the exact reconstruction of the detailed structure of a *specific* string. These notions of computational complexity are not well suited for quantifying the difficulty in modeling dynamical systems; there, one is interested in the entire set of allowed trajectories rather than the detailed structure of a particular output string.

The presence of the unstable periodic orbits provides a treelike skeleton on which the multitude of possible motions can be hierarchically organized.

III. EXAMPLES

The most studied systems which are well represented by binary symbolic dynamics are the one-dimensional unimodal maps,<sup>18</sup> specifically the quadratic map

$$x_{n+1} = 1 - ax_n^2 \tag{2}$$

on the interval  $[-1, 1]$  with  $0 < a \leq 2$ . The symbols 0 and 1 represent phase-space coordinates below the critical point of the map and above it, respectively. A code  $\eta$  on the unit interval can be associated with the forward symbolic itinerary  $\{S_i\}$  of each point on the interval  $[-1, 1]$  as follows:

$$\eta = \sum_{i=0}^{\infty} \sigma_i 2^{-i-1} \text{ with } \sigma_i = \left[ \sum_{j=0}^i S_j \right] \bmod 1. \tag{3}$$

If the parameter  $a$  is chosen so that a strange invariant set exists, the maximum value of  $\eta$  is given by the itinerary of the first iterate of the critical point, while the minimum value of  $\eta$  is given by its next iterate.<sup>18</sup> In fact, the points on the strange invariant set are those with  $\eta$  values between those of the minimum and maximum, provided all their iterates also have  $\eta$  values in this range. Thus, given the forward symbolic itinerary of the critical point (the *kneading sequence*) to arbitrary length, it is possible to determine the set of allowed periodic sequences to any given length. As will be demonstrated in the following examples, a periodic kneading sequence defines a Markov partition for the invariant set giving rise to a simple grammar. In the examples below, two parameter values of the quadratic map (2) are approached, one in which the kneading sequence is eventually periodic and the other in which it is aperiodic.

A. Period-3 band merging

Within the chaotic regime of the map (2) there are regular regions; the largest of these is the period-3 window

which lies approximately in the range  $1.75 \leq a \leq 1.78$ . At the lower end of this window a pair of period-3 orbits is produced via a tangent bifurcation; the stable one subsequently undergoes a series of period-doubling bifurcations whose accumulation point is  $a \approx 1.78$ . Beyond the accumulation point, chaotic behavior is confined to three disjoint bands which suddenly widen and merge at  $a \approx 1.79$  (the period-3 band-merging parameter value). This phenomenon has been referred to as an *interior crisis*<sup>19</sup> since an unstable periodic orbit within the basin of attraction of the chaotic attractor collides with the attractor, causing a sudden change in the size of the attracting set. The unstable orbit involved in this crisis is the period-3 orbit created through the tangent bifurcation at  $a \approx 1.75$ .

At the crisis parameter value, the fourth iterate of the critical point falls on the unstable period-3 orbit, so its kneading sequence is  $100(101)^\infty$ . We approach crisis from above, via parameter values possessing periodic kneading sequences of the form  $100(101)^n 1C$ , where  $C$  denotes the critical point and  $n$  increases from 0. As  $n \rightarrow \infty$  the crisis parameter value is approached monotonically. At each  $n$ , although the attractor is a *superstable* periodic orbit (maximum stability), there exists a strange invariant repelling set lying within the interval  $[1-a, 1]$ . The boundaries of a Markov partition for the repeller and its underlying dense set of periodic orbits are given by the members of the superstable orbit.

In the following, the complete tree corresponding to the parameter value possessing a superstable period-8 orbit with symbol sequence  $1001011C$  ( $n=1$ ) is constructed. Each of the seven elements of the Markov partition shown in Fig. 3(a) has at most two preimages (on opposite sides of the critical point) which are given by

$$1 \rightarrow 7, \quad 2 \rightarrow 6, \quad 3 \rightarrow 1, 6, 4 \rightarrow 1, 5, \\ 5 \rightarrow 2, 5, \quad 6 \rightarrow 2, 4, \quad 7 \rightarrow 3, 4.$$

These relations are represented graphically on the seven-node graph shown in Fig. 3(b). The directed links pointing towards the preimages are labeled by 0 or 1, depending on whether the preimage lies to the left or right of the

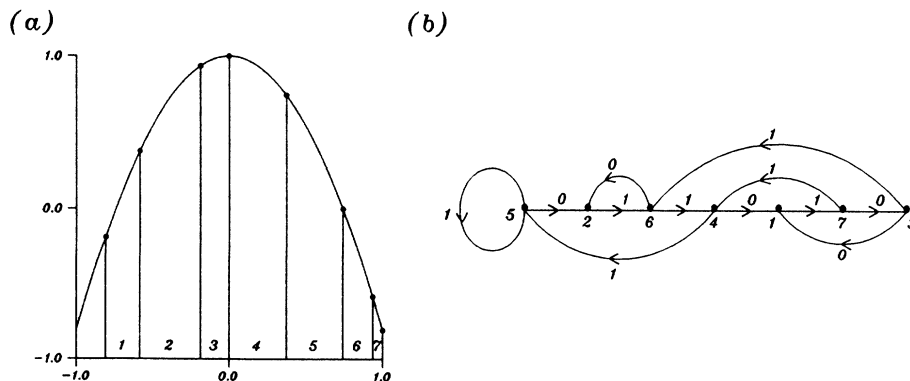


FIG. 3. (a) Markov partition for the map (2) at  $a = 1.81000 \dots$  where it possesses a superstable period-8 orbit. The partition elements are labeled by the number 1-7, while the cycle points are denoted by heavy dots. The corresponding directed graph is shown in (b) with nodes labeled by the partition elements of (a).

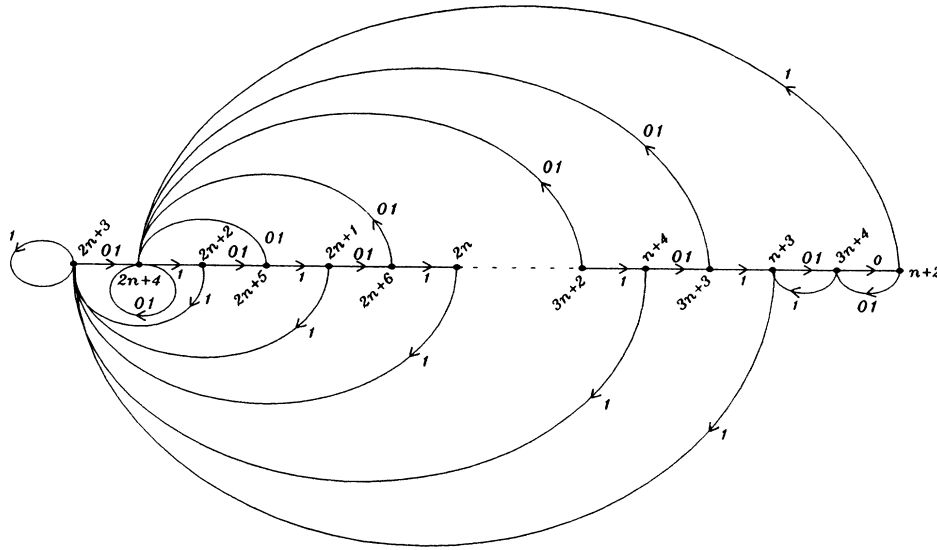


FIG. 4. General directed graph arising from the map (2) at a parameter value where it has a superstable period  $3n + 5$  orbit ( $n$  large). For convenience, some of the nodes have been eliminated in favor of links labeled with a string of two symbols. The dashed line represents the missing part of the graph which follows the same pattern as shown.

critical point, respectively. A directed path in the graph which ends at the starting node singles out a periodic point lying in the corresponding element of the Markov partition. For example, the path on the graph of Fig. 3(b),  $1 \rightarrow 7 \rightarrow 3 \rightarrow 6 \rightarrow 4 \rightarrow 1$  corresponds to the period-5 point in the leftmost partition element of Fig. 3(a) with symbol sequence 01101. Note that since the graphs are drawn with the links directed towards the preimages, the forward symbol sequence is obtained from reversing the order of the symbols along its path.

All the periodic points in partition element 4 are contained in the regular expression

$$[11(001)^*0 + 1(10)^*101(001)^*0 + 11(01)^*01^*1]^*, \quad (4)$$

producing a complete ternary tree arrangement. Not all periodic orbits of the system are present on the tree, since some may never visit the specific partition element during their cycles. For example, the fixed point denoted by the symbol sequence 1, which is found in partition element 5, is not present in the above ternary tree. In any case, its existence is deduced from the presence of its preimages on the ternary tree, e.g.,  $101^*$  and  $10101^*$ . The fact that arbitrary repetitions (the  $*$  operator) of 1, 01, and 001 are present in the ternary tree of expression (4) implies that these are allowed periodic orbits of the system even though they do not enter partition element 4 at any point along their cycle. All other periodic orbits of the system visit partition element 4 at least once during each cycle. In fact, the number of periodic points of a given orbit that are included on the tree is given by the number of times it visits the partition element in question, during its

cycle. Due to this difference in the number of appearances of various periodic orbits on the tree, the topological entropy is not immediately available from the above complete tree construction. A complete tree with possibly less branching is produced if the construction carried out above is repeated using an alternate starting node. It can be easily checked that these alternate trees have internal branchings, resulting in a total number of three branchings when they are taken into consideration.

At this point, it is necessary to check how the branching of the tree grows as we approach the crisis parameter value. The allowed set of unstable periodic orbits at the parameter value corresponding to a superstable orbit of symbol sequence  $100(101)^n1C$ , is identical to the set of unstable periodic orbits at crisis if only orbits up to length  $3n + 4$  are considered. The kneading sequences at both these parameter values are identical up to this length, resulting in equivalent sets of allowed  $\eta$  codes [defined in Eq. (3)] up to this length. If one considers only orbits of period-7 ( $n = 1$ ) or less, in the ternary tree in expression (4), one finds identically the orbits present at crisis.

For arbitrarily large  $n$ , the directed graph of Fig. 3(b) describing the grammar of the repeller generalizes to the one shown in Fig. 4. Notice that some of the links have a string of two symbols attached to them rather than just 0 or 1. These longer strings arise due to the elimination of the first  $n + 1$  nodes from the graph, which are exactly the ones having only a single preimage. Since we are only concerned with the actual strings accepted by the graph and not the specific node structure, the form of Fig. 4 is more convenient for our purposes. Using node  $2n + 4$  as the starting node, one obtains a complete tree for arbitrary  $n$  which can be denoted by the regular expression

$$[10 + 10(101) + 10(101)^2 + \dots + 10(101)^{n-1} + 101^*11 + 101^*11(101) + 101^*11(101)^2 + \dots + 101^*11(101)^{n-2} + 101^*1(1(100)^*10)^*1(101)^{n-1} + 10((100)^*101)^*(101)^n]^* . \tag{5}$$

Although the above expression describes a tree where every branch splits into  $2n + 1$  new branches, the orbits up to period  $3n + 4$  are exactly those included in the binary tree denoted by the expression

$$[10(101)^* + 101^*11(101)^*]^* , \tag{6}$$

which is exactly the tree obtained in the limit  $n \rightarrow \infty$  of expression (5). In other words, a binary tree is sufficient in order to fully describe the cycles up to an arbitrary length at the crisis parameter value, thus endowing it with grammatical complexity  $C_0 = 0$  according to relation (1). The consideration of different starting nodes in Fig. 4 again leads in the limit of large  $n$  to a finitely branched complete tree similar to that of expression (6).

The quadratic map at crisis can be approached along many other sequences of parameter values, but the claim is that all these methods will also lead to a zero complexity grammar. This can be understood from the fact that the mapping at crisis itself possesses a Markov partition whose boundaries are given by the critical point and it iterates (six elements in total). The corresponding graph is shown Fig. 5 and its most noticeable feature is the existence of two disjoint invariant sets. Periodic orbits entering element 2 will subsequently enter only into element 5 before returning back into element 2. All other period orbits visit neither element 2 nor element 5. In fact, the chaotic attractor for period-3 band merging lies within the elements 1, 3, 4, and 6 of the markov partition, while a chaotic repeller exists within the elements 2 and 5. Almost all initial points in elements 2 and 5 eventually fall on the attractor so that the repelling part of the graph in Fig. 5 can be considered as a transient of the motion on the attractor. The grammar is simple for both strange sets and can be expressed as a binary tree in either case; for the repeller it is  $(1 + 10)^*$ , while for the attractor it is  $(100 + 101)^*$ . The binary tree in expression (6) includes only the orbits on the repeller, since partition element  $2n + 4$  of Fig. 4 is on the repeller. The limiting

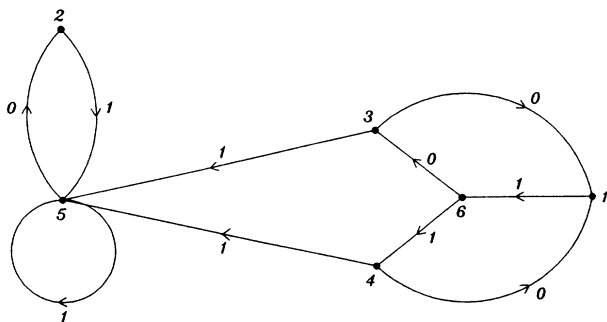


FIG. 5. Directed graph describing the grammar of the attractor (right) and repeller (left) at the period-3 band merging parameter of mapping (2) at  $a = 1.78 \dots$

grammar of the three-band attractor at crisis can be obtained by considering node  $n + 2$  say, of Fig. 4 as the starting node for the complete tree construction.

At the band merging parameter value, an unstable period-3 orbit lies on the boundary point of each of the three bands. Infinitesimally above this parameter, the period-3 orbit lies in the region previously occupied by the repeller, and all the trajectories on what was previously the repeller become accessible from the region which was previously occupied by the attractor. In this way, the attractor and repeller coalesce to produce a single larger attractor, whose grammar can be described by a graph (or a limit of graphs) without transient parts. Below band merging but near it, there are transients in a graph describing the grammar, which again correspond to a strange repeller located between the attractive bands.

All the grammars that were discussed in this section turned out to be simple. By similar means, it can be shown that the grammatical complexity is, in general, zero for any parameter value of a unimodal map having a periodic or preperiodic kneading sequence. In the following a mapping with an aperiodic kneading sequence is explicitly considered.

**B. Aperiodic kneading sequence**

The quadratic map (2) at parameter value  $a_\infty = 1.7103989 \dots$  has an aperiodic kneading sequence whose code  $\eta$  defined in (4) takes on the value of the golden mean  $\omega_G = 0.618 \dots$ . The actual kneading sequence can be generated using a hierarchical construction rule<sup>15</sup> leading to an infinite sequence which is invariant under the block renaming operator:

$$\alpha \rightarrow \alpha\beta, \quad \beta \rightarrow \alpha\beta\beta , \tag{7}$$

where  $\alpha = 011$  and  $\beta = 01111$ . The first few levels of construction of the first iterate of the kneading sequence are

$$\begin{aligned} &\alpha \\ &\beta \\ &\alpha \beta \\ &\alpha\beta \beta \\ &\alpha\beta \alpha\beta\beta \\ &\alpha\beta\alpha\beta\beta \alpha\beta\beta \\ &\alpha\beta\alpha\beta\beta \alpha\beta\alpha\beta\beta\alpha\beta\beta . \end{aligned} \tag{8}$$

The most natural approach to the parameter value possessing the above aperiodic kneading sequence is through parameter values with superstable orbits of lengths  $F_n$ , the Fibonacci numbers. The itinerary of the superstable approximant of length  $F_n$  is given by the  $(n - 3)$ rd level of the construction in (8), with the final  $\beta$  being replaced with the string  $011C1$ . The Markov partition for the strange repelling set is again given by the points of the superstable orbit. In the limit  $n \rightarrow \infty$  the strange repelling

set changes its stability to emerge as the sole attractor of the system. Unlike the monotonic approach to the interior crisis discussed above, the approach via the Fibonacci approximants is along stable windows in parameter space which alternate on both sides of  $a_\infty$ .

The preimages of the  $F_n - 1$  Markov partition elements (numbered in increasing order from left to right) at the superstable  $F_n$  parameter value are given by

$$i \rightarrow \begin{cases} F_n - i & \text{if } i \in [1, F_{n-2}] \\ F_{n-1}, i - F_{n-2} & \text{if } i \in (F_{n-2}, F_{n-1}] \\ F_{n-3}, 2F_{n-1} - i & \text{if } i \in (F_{n-1}, F_n - 1] \end{cases}$$

As can be observed from these relations, only the last  $F_{n-1} - 1$  of the partition elements have two preimages. For convenience, the first  $F_{n-2}$  partition elements are not represented on the transition graph of Fig. 6; instead some links are labeled with two symbols as was the case in Fig. 4. The nodes labeled in Fig. 6 have also been renumbered for convenience by subtracting  $F_{n-2}$  from each.

All the intermediate nodes on the horizontal line of Fig. 6 have a link emanating from them towards either the lower node ( $F_{n-3}$ ) or the upper one ( $F_{n-2}$ ). In the limit of large  $n$ , the number of links approaching the lower node is a factor of  $\omega_G$  smaller than those approaching the upper node. The periodic orbits that enter element  $F_{n-2}$  only once during their cycle can be determined from the graph of Fig. 6 (see Appendix B for details). After a single iteration, all the periodic points found in element  $F_{n-2}$  enter the same *single* partition ele-

ment whose right-hand boundary is given by the critical point. For convenience, we choose to construct the building blocks of the orbits entering this partition element, which are given by

$$\begin{aligned} & 01 \\ & 01111^* \\ & 01\Delta_i\Delta_{i-1}\cdots\Delta_1, \quad (\forall i < N) \\ & 01111^*\Delta_i\Delta_{i-1}\cdots\Delta_1 \text{ for } \Delta_{i+1}=\alpha \text{ or } i=N-1 \quad (9) \\ & 0111\Delta_i\Delta_{i-1}\cdots\Delta_1 \text{ for } \Delta_{i+1}=\beta \\ & 0111111^*\Delta_i\Delta_{i-1}\cdots\Delta_1 \text{ for } \Delta_{i+1}=\beta \end{aligned}$$

where  $N = F_{n-3}$  and  $\Delta_1\Delta_2\cdots\Delta_N$  is the symbol sequence of the second iterate of the critical point at the super stable  $F_n$  parameter value.  $\Delta_i$  takes on the value  $\alpha$  or  $\beta$  according to the hierarchical construction in (8), while  $\Delta_N = 011C1$ .

The number of  $\beta$  blocks appearing in the itinerary  $\Delta_1\cdots\Delta_N$  of the critical point is  $F_{n-4} - 1$ , as can be deduced from the inflation rule (7) used for constructing the itineraries. It follows that the number of building blocks  $k(F_n)$  necessary to describe the periodic orbits up to period  $F_n$  at the parameter value  $a = a_\infty$  can be obtained by summing the number of regular expressions appearing in each line of list (9):

$$k(F_n) = 1 + 1 + (F_{n-3} - 1) + F_{n-5} + (F_{n-4} - 1) + (F_{n-4} - 1) = F_{n-1} - 1. \quad (10)$$

In the limit of  $n \rightarrow \infty$ ,  $F_{n-1}/F_n$  approaches the golden mean, yielding  $C_0 = \omega_G \approx 0.618$ . Thus the grammar at  $a_\infty$  is complex; new building blocks are asymptotically al-

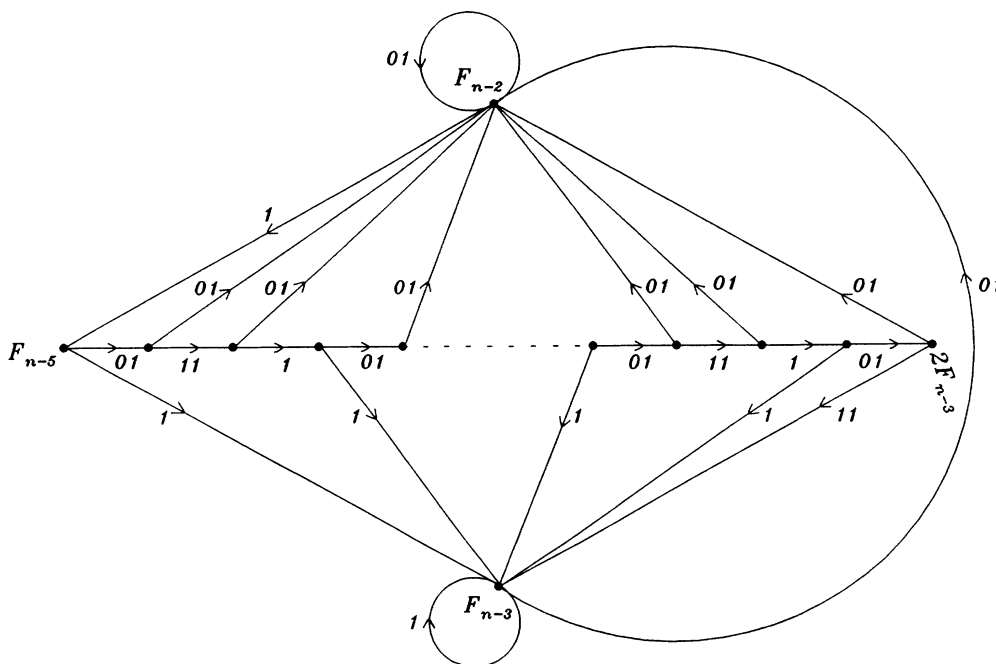


FIG. 6. General directed graph of the repeller corresponding to a parameter value of mapping (2) possessing a superstable orbit of length  $F_n$ . These are the approximants to the grammar of the attractor at  $a_\infty \approx 1.71039$ . Most of the nodes are not labeled and some are replaced by labeling links with two symbol strings. Again, the dashed line corresponds to a missing section of the graph with the same general form as that shown.

ways necessary in order to provide an exact characterization of longer-allowed orbits. The necessity for building blocks of increasing length can be deduced from analyzing a time series at  $a = a_\infty$ . Since a single building block may consist of a family of orbits of increasing length, its length is considered to be the number of 0 and 1 symbols present in its representation as a regular expression. Figure 7 is a plot of the number of building blocks of length less than  $l$  present in a numerically obtained time series at  $a = a_\infty$  of length  $10^6$ . It is apparent from the straight-line fit with slope  $C_0 = 0.618 \pm 0.002$  that all the building blocks up to length 50 are present in the time series.

We briefly discuss the possibility of approaching  $a_\infty$  via complete trees alternative to the one composed of the building blocks in (9). First, consider using a particular node  $i$  lying on the horizontal line of the graph shown in Fig. 6 as a possible starting node for a complete tree construction. Each building block is obtained by first following a horizontal path of arbitrary length to the right and then turning either up or down (only one of these directions is legal except for the last node on the line where either one is allowed) and following the unique path to node number  $F_{n-2}$ . Then a subtree of all the blocks of (9) except for those that go through node  $i$  appears in the building block. Following the subtree, the unique shortest path connecting node  $F_{n-2}$  to node  $i$  completes the building block. The number of building blocks obtained using the above procedure depends upon where on the horizontal line of Fig. 6, node  $i$  lies. The further it lies to the left, the more building blocks it has and their number is given by the number of nodes to its right increased by two. Each of these building blocks includes an identical subtree with a number of branches equal to the number of nodes on the horizontal line to the left of  $i$  increased by one. Taking the branching within the building blocks into account, by adding the number of “+” operations in

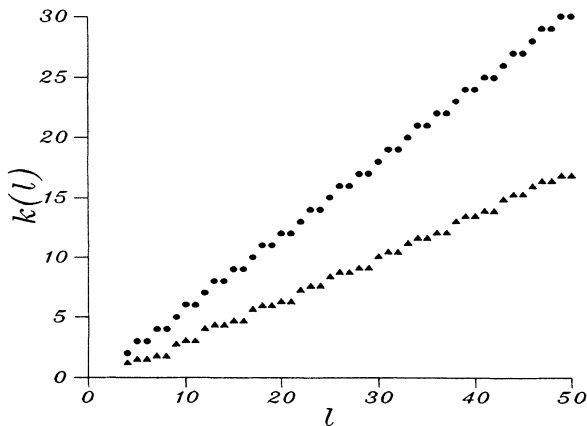


FIG. 7. Total number  $n(l)$  of building blocks up to length  $l$  for the map (2) at  $a = a_\infty$  are shown as circles. Only the building blocks appearing in a numerical time series of length  $10^6$  are counted. The slope is given by  $0.618 \pm 0.001$  in good agreement with  $C_0 = \omega_G$ . The triangles represent the approximants to  $lC_1^{(l)}$  obtained by considering only blocks up to length  $l$  in the same time series. The slope is given by  $C_1 = 0.354 \pm 0.002$ .

the subtree to the number of building blocks, Eq. (10) is confirmed for any choice of starting node on the horizontal line of Fig. 6. Similar considerations yield the same result for node  $F_{n-3}$ , which is the only other node that does not lie on the horizontal line of Fig 6.

#### IV. GENERALIZED COMPLEXITIES

In Secs. II and III we were concerned only with reconstructing the allowed orbits of a system, irrespective of their probability of occurrence in a typical time series. A long trajectory can be considered as motion through the set of periodic orbits obtained by uniquely parsing the trajectory according to the building blocks of the system. The frequency of occurrence of each building block is governed by the distribution of the invariant measure on the strange set. It is conceivable that only a finite number of building blocks is sufficient for reconstructing all trajectories of a system occurring with a probability greater than some threshold, even through the system may be grammatically complex. In this section, we introduce quantities which indicate how well a complex grammar can be approximated by its simple grammatical approximants when the distribution of the invariant measure on the strange set is taken into account.

Typically, in a chaotic system the probability to observe a particular symbol sequence decreases exponentially with the length of the sequence. In the special case where the probability distribution over all symbol sequences of a given length is uniform, we naturally expect any measure-dependent complexity to reduce to the grammatical complexity. In order to measure the nonuniformity in the probability distribution on the building blocks, the spectrum of generalized complexities is introduced in much the same way as the Rényi dimensions and entropies<sup>20</sup> in the generalizations of the topological definitions of dimension and entropy, respectively. The extension of  $C_0$  to a function  $C_q$  for all real  $q (q \neq 1)$  is given by

$$C_q = \lim_{N \rightarrow \infty} \frac{1}{N} \left[ \sum_i p_i^q \right]^{-1/(q-1)}, \quad (11)$$

where the sum goes over all the building blocks with length up to  $N$  (there are  $C_0 N$  of these in the limit of large  $N$ ) and  $p_i$  represents the probability of a particular building block. It can be easily checked that a uniform probability distribution over all  $C_0 N$  building blocks results in  $C_q = C_0$  for all  $q$ , as expected. In general,  $C_q$  is a monotonically decreasing function of  $q$ , which is bounded from above and below. The lower bound  $C_\infty$  gives the asymptotic growth rate of the predominant (highest probability) building blocks necessary for a reconstruction of a chaotic trajectory. Due to the presence of at most a number linear in  $N$  building blocks in the sum of expression (11), the linear scaling of the sum with increasing  $N$  is the relevant quantity to extract. The analogous expressions used for defining the generalized entropies and dimensions are obtained by taking the logarithm of a sum similar to the one in Eq. (11), since in those cases the sum is over an exponential number of terms in  $N$ , where  $N$  is the length of a trajectory. In fact, all the orbits appearing



on the  $N$ th level of a tree are included, rather than only the top level of the tree (the building blocks) as is the case for the complexities.

The precise definition of the probabilities that enter into Eq. (11) is now explained. A building block  $B$  is in general a family of periodic orbits  $\{B_i\}$  of varying unbounded lengths. In order to determine their total probability, a trajectory following the stationary distribution is uniquely parsed into substrings corresponding to orbits contained within the building blocks of the system. The probability of building block  $i$ ,  $p_i$ , is then given by

$$p_B = \frac{c}{n_B} \lim_{N_t \rightarrow \infty} \sum_i \left( \frac{N_{B_i}}{N_t} \right)^{1/l_{B_i}}, \quad (12)$$

where  $c$  is a normalization constant and  $n_B$  is the number of distinct member orbits  $B_i$  of building block  $B$  which were extracted from the time series. The total number of pieces in which the parsing of the real trajectory results is  $N_t$ , while  $N_{B_i}$  is the number of times orbit  $B_i$  appears. The frequency in which  $B_i$  is encountered is raised to the power of its inverse period  $1/l_{B_i}$ , in order to obtain a probability per single symbol. The probability to observe a string of length  $l$  scales as  $e^{-\alpha l}$  for some positive  $\alpha$ , and we are only interested in considering the length independent weight  $e^{-\alpha}$  of each orbit. The metric complexity  $C_1$  is defined by taking the  $q \rightarrow 1$  limit of relation (11) to obtain

$$C_1 = \lim_{N \rightarrow \infty} \frac{1}{N} \exp \left[ - \sum_i p_i \ln p_i \right]. \quad (13)$$

As an example of the complexity spectrum, we have calculated the probabilities of the various building blocks of the map (2) at parameter value  $a_\infty$  by parsing a numerically generated time series of length  $10^8$  with the building blocks in list (9). For each  $q$ , the value  $NC_q^{(N)}$  scales linearly with  $N$  enabling a determination of  $C_q$  from the slope (see Fig. 7). The approximants  $C_q^{(N)}$  are those obtained using solely the blocks with length less than  $N$ . Our results for very large  $N$  ( $> 50$ ) do not follow the expected asymptotics due to the limited size of the time series that was used. In addition, the parameter value  $a_\infty$  cannot be pinpointed exactly, so that the time series was generated at a nearby parameter value with building blocks identical to those of  $a_\infty$  at least to length 50.

The resulting spectrum of generalized complexities obtained by considering building blocks up to length 50 is shown in Fig. 8. Rather than plotting  $C_q$ , we plot  $\tau(q) \equiv (q-1)C_q$  in order to make the connection with the thermodynamic formalism of dynamical systems<sup>21,22</sup> more apparent.  $\tau(q)$  is analogous to the free energy and any singularity in this function signifies a phase transition,<sup>23</sup> indicating the presence of nongeneric scalings in the probabilities of Eq. (12) with increasing maximum block length. From the graph of Fig. 8, there seems to be no such singularity, indicating that each of the block probabilities  $p_i$  scales in a similar fashion with increasing length of the longest building block considered. Generically, we expect to encounter nonanalytic behavior in the spectrum of generalized complexities of other systems.

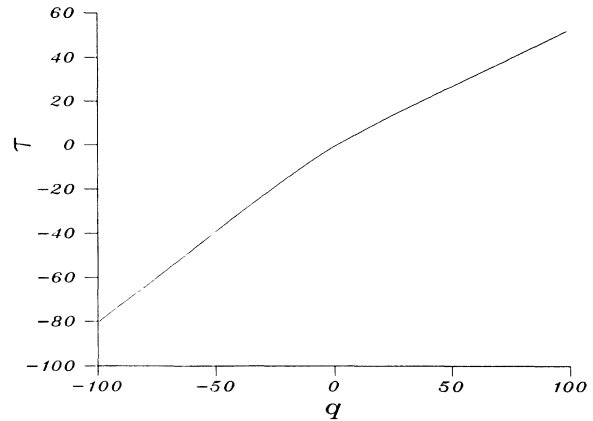


FIG. 8. Generalized complexity spectrum  $C_q(q-1)$  for the map (2) at  $a = a_\infty$ . The probabilities for the various building blocks were extracted from a numerical time series of length  $10^{10}$ . The convergence of the spectrum with the length of the run is quick.

The probability distribution of the invariant measure on the set of building blocks of a complex grammar characterized by the generalized complexities would be sufficient in reconstructing the motion of a chaotic trajectory, provided correlations were absent among the building blocks. Typically, the correlation function decays exponentially for chaotic systems, or by a power law for intermittent cases. Correlations present in a time series are reflected in the convergence rates of the metric entropy and its Rényi generalizations.<sup>12,24,25</sup> Consider, for example, the definition of the metric entropy as

$$K = \limsup_{m \rightarrow \infty} \frac{1}{m} K^{(m)}, \quad (14)$$

where the block entropies  $K^{(m)}$  are given by

$$K^{(m)} = - \sum_{\sigma_m} P(\sigma_m) \ln P(\sigma_m), \quad (15)$$

and the sum is over all orbits  $\sigma_m$  of length  $m$ . The convergence of the right-hand side of expression (15) to  $K$  has been used to introduce the *effective measure complexity*<sup>12</sup> defined as

$$\mathcal{C}_{\text{EMC}} = \lim_{m \rightarrow \infty} (K^{(m)} - mK). \quad (16)$$

The block entropies grow monotonically with  $m$ , and on division by  $m$  they usually converge to  $K$  at a rate proportional to  $1/m$  for chaotic systems.<sup>12,24</sup> In addition, the consecutive differences of the truncated entropies in Eq. (15) decay monotonically to the metric entropy either exponentially in generic cases, or as a power law for intermittent cases.<sup>24</sup> These differences of consecutive block entropies,  $\Delta K^{(n)}$ , are essentially conditional entropies, whose convergence rate somewhat reflects the degree of stochasticity or randomness in the system. In fact, for 1D maps the exponential convergence rate exhibits a local maximum at the parameter value corresponding to fully developed chaos, while for intermittent cases the

convergence rate is slower than exponential.<sup>24</sup>

In order to obtain an entropy-independent quantification of the correlations in a chaotic times series we study the convergence of the generalized complexities ob-

tained at successively lower levels of the complete tree construction. Using only the words appearing on the  $m$ th level of the tree, one obtains the metric complexity at this level as

$$C_1^{(m)} = \lim_{N \rightarrow \infty} \frac{1}{N} \exp \left[ - \sum_{b_1, \dots, b_{m-1}} p(b_1, \dots, b_{m-1}) \sum_{b_m} p(b_m | b_1, \dots, b_{m-1}) \ln p(b_m | b_1, \dots, b_{m-1}) \right], \quad (17)$$

where all the building blocks  $b_i$  up to length  $N$  are included in the sums. The joint probability of observing a string of  $m$  consecutive building blocks  $p(b_1, \dots, b_m)$  is normalized with respect to its length as in Eq. (12). The conditional probabilities  $p(b_m | b_1, \dots, b_{m-1})$  are defined in the usual way as a quotient of joint probabilities. It can be easily shown that the above expression for  $C_1^{(m)}$  is equivalent to consecutive differences of the *block complexities*:

$$S^{(m)} = \exp \left[ - \sum_{b_1, \dots, b_m} p(b_1, \dots, b_m) \ln p(b_1, \dots, b_m) \right], \quad (18)$$

where the similarity to the block entropies in Eq. (15) is apparent.

The convergence of the metric complexities will in general be faster than that of the metric entropies due to the fact that some of the correlations are incorporated within the indecomposable building blocks. Therefore one expects that generically the metric complexity at level  $m$ ,  $C_1^{(m)}$  also converges exponentially in the limit of large  $m$ . Since the building blocks are the construction units necessary for a hierarchical encoding of a chaotic system, the convergence rate of many dynamical invariants such as entropies, dimensions, and Lyapunov exponents may be improved through their estimation at successive levels of the complete tree of building blocks.

In practice, it is difficult to calculate the metric complexities  $C_1^{(m)}$  past  $m=2$  or 3 for a complex grammar directly from a time series, due to the inaccuracies encountered in an attempt to extract high-order joint probabilities from a reasonable length time series. For the case of the 1D map possessing an aperiodic kneading sequence whose generalized complexities are shown in Fig. 8, we have managed to calculate  $C_1$  for the second level of the tree. Within our accuracy,  $C_1^{(1)} = C_1^{(2)}$ , which is expected due to the exponential decay of correlations in this case. In order to examine the decay of the correlations between building blocks more accurately, we study systems with a finite number of building blocks whose grammar is simple. In any case, the decay of the correlations between blocks can be analyzed via the convergence of the conditional entropies calculated down the levels of the complete tree of building blocks.

As a simple example, consider the first period-2 band splitting point<sup>26</sup> of the quadratic map (2) at the parameter

value  $a = 1.5436 \dots$ . The topological entropy is  $\ln(\omega_G^{-1})$  due to the exclusion of all orbits with two or more consecutive 0's. A Markov partition with three elements (bounded by the critical point and its three iterates) exists for the attractor. All the periodic orbits present in the system can be obtained from combinations of the building blocks 10 and 11. Note that the fixed point labeled 1 lies on the boundary between two Markov partition elements and therefore appears as 11 in the tree. In Fig. 9, the convergence of consecutive conditional entropies  $\Delta K^{(m)}$  is shown with respect to the level  $m$  of the complete binary tree of building blocks. Thus at level  $m$  of the complete tree, orbits are specified by  $2m$  of the basic alphabet symbols. Results for levels higher than 6 are inaccurate, once again due to the limited size ( $10^8$  steps) of the time series. As can be seen from Fig. 9, the conditional entropy converges exponentially as  $e^{-\gamma m}$  with the slope given by  $\gamma = 1.33 \pm 0.02$ . The actual metric entropy approximants calculated in terms of the basic symbols 0 and 1 converge more slowly with a decay constant equal to  $\frac{1}{2}\gamma$ .<sup>24</sup> Such accelerated convergence of quantities calculated in terms of the building blocks rather than the alphabetic symbols is expected in general.

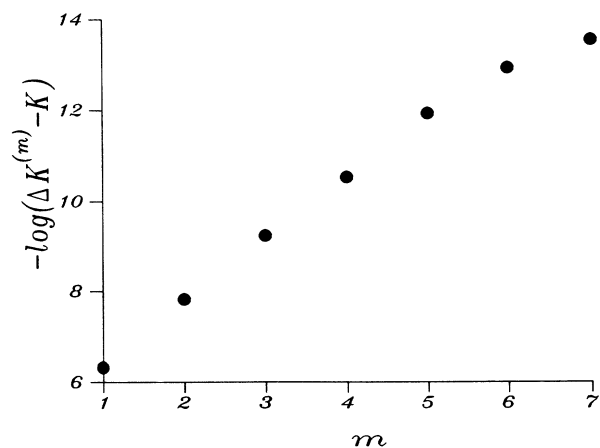


FIG. 9. Convergence of the conditional entropies calculated from a time series of length  $10^8$  in terms of the two building blocks of the map (2) at the first band splitting point  $a \approx 1.5436$ . The logarithm of the difference between the conditional entropy  $\Delta K^{(n)}$  and its limiting value  $K$  is plotted vs the level number. The slope is given by  $1.33 \pm 0.02$  from considering the first six levels where the converged entropy in terms of the building blocks is  $K = 0.68435$ .

## V. SUMMARY

Most studies on chaotic systems are concerned with extracting dynamical information such as dimensions and entropies from a wide range of physical phenomena. The convergence properties of such calculations are dependent on the complexity of the dynamical system. Low-order data may provide an adequate encoding of the properties of a simple system, while it may be virtually useless in the case of a complex system. By studying systems endowed with symbolic dynamics, we have quantified the difficulty in hierarchically encoding the topological characteristics of a dynamical system via the introduction of the grammatical complexity, which was subsequently generalized to include metric properties. These were taken into account by an evaluation of the nonuniformity in the distribution of the invariant measure over the building blocks, as well as a consideration of the correlations between these blocks.

The building blocks and the complete tree they generate provide a useful framework in which invariant dynamical quantities may be calculated and analyzed. Until now, the level of a hierarchical organization of the periodic orbits was given by their length. The fact that the building blocks are indecomposable basic units from which a chaotic trajectory can be reconstructed strongly indicates that the complete tree they generate may be used as a hierarchical framework that can accelerate the convergence in the evaluation of dynamical invariants. Given a time series, there is still no effective general procedure to extract the set of building blocks directly from it. Practically, we are usually only interested in organizing orbits whose probability is greater than some threshold value and whose length is less than some maximum observable length. Extracting the building blocks from a time series, in this limited sense, is possible but may not always be computationally feasible.

Although in this paper we have only considered examples derived from 1D maps, the procedure can be generalized to higher-dimensional systems provided a good symbolic description exists. For example, in 2D Hénon-like systems,<sup>27</sup> it has been conjectured that two symbols are sufficient in order to encode the dynamics faithfully.<sup>28</sup> A parameter value possessing an infinite grammar (words of arbitrary length are disallowed) can be approached along parameter values possessing a finite grammar, such as the set of parameter values corresponding to the mutual tangent bifurcations of two pairs of periodic orbits; a couple of these parameter values have been studied in Refs. 29 and 30. At all such parameter values, the grammar can be represented by a finite directed graph. This picture holds for reasonably large dissipation values  $b$  of the Hénon map;<sup>29</sup> there, an approach to an arbitrary parameter value can be made along parameter values described by these particular finite grammars.

The scope of the notion of complexity presented here is much wider than solely dynamical systems exhibiting low-dimensional chaos. For example, it can be directly applied to a study of the spatial configurations of cellular automata limit sets. It is known that the possible spatial strings that can be obtained after  $n$  time steps in the evo-

lution of a 1D cellular automaton form a regular grammar. In the limit of  $n \rightarrow \infty$  the language may no longer be regular, and may be a member of any of the higher-level languages in the Chomsky hierarchy.<sup>31</sup> In fact, the limit grammar may not even be in the class of recursively enumerable languages.<sup>10</sup> By studying the regular language grammars approaching a cellular automata limit set, the grammatical complexity introduced here and its generalizations can be deduced. Their values may provide additional characteristics for improved classification schemes of cellular automata rules.

## ACKNOWLEDGMENTS

We thank R. Badii, J.-P. Eckmann, and C. Langton for valuable discussions. One of us (D. A.) thanks Doyné Farmer and both the T-13 group and the Center for Non-linear Studies for their hospitality at Los Alamos National Laboratory, where part of this work was completed. I. P. acknowledges the partial support of the U.S.–Israel Binational Science Foundation and the Israel Academy of Sciences, the commission for basic research.

## APPENDIX A

In this appendix, we demonstrate that the grammatical complexity  $C_0$ , defined in Eq. (1), is bounded from above by the value 2 for binary symbolic dynamics. First, a sequence of directed graphs approximating a grammar which gives rise to two building blocks at each length is constructed. The  $n$ th level directed graph approximation to this limit grammar is shown in Fig. 10. The links can be labeled arbitrarily by 0's and 1's, provided that any two links emanating from the same node do not have the same label. At each successive level in this hierarchical construction, an additional node is added to the horizontal line of the graph. Considering node  $A$  as the start node, one sees that each node on the horizontal line contributes two building blocks; there are exactly two choices of preimages for node  $A$  (either  $B$  or  $C$ ), each producing a building block whose path goes over to a given node on the horizontal line and then returns in one step to node  $A$ . The total number of building blocks for such a graph with  $n$  nodes is  $2(n-1)$ , apparently leading

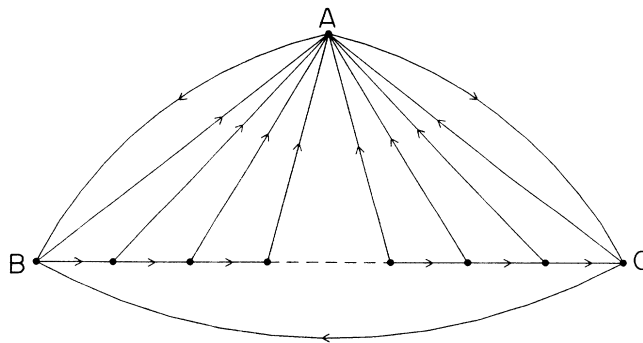


FIG. 10. General form of a directed graph having  $2(n-1)$  building blocks in the presence of  $n$  nodes, yielding an upper bound of 2 for the grammatical complexity of binary systems.

to  $C_0=2$ . On the other hand, since each node in Fig. 10 has two preimages, the graph accepts all possible strings of 0's and 1's in the limit of an infinite-size automaton. Complex grammars can arise only if some links in the graph of Fig. 10 are removed, demonstrating the conclusion that the grammatical complexity is bounded from above by  $C_0=2$ .

It will now be shown that any system with  $C_0=2$  has a topological entropy of  $\ln 2$  and that increasing the grammatical complexity any further would lead to a larger value of the topological entropy, which is of course disallowed for binary symbolic dynamics. Consider a system with two building blocks at each length which is longer than some minimum length  $k$ . We will take  $k=2$  for simplicity, although the same result can be obtained for any finite  $k$ . By induction, we show that the number of periodic points of length  $n$  scales like  $2^n$  for  $n \gg 2$ . Say at  $n=n_1$  the number of periodic points is greater than  $\alpha 2^{n_1}$  (this is certainly true for small  $n_1$  since we can choose the constant  $\alpha$  accordingly). Periodic points of length  $n=n_1+2$  can be obtained by adding either of the two building blocks of length 2 to each of the orbits of length  $n_1$ . In addition one can take each orbit of length  $n_1$  and replace its last building block by one of the two blocks whose length is two bits longer. Note that all of the points constructed are different since each periodic point has a unique position on the complete tree of building blocks. In this way, we produce  $\alpha 2^{n_1+2}$  periodic points of length  $n_1+2$ , thus proving that the topological entropy is at least  $\ln 2$ .

A similar induction can be used to prove that the topological entropy is at least  $\ln 2$  also when the minimum length of twin building blocks is  $k > 2$ . For cases with  $C_0 > 2$ , i.e., on the average more than two building blocks at each length, one can similarly show that the topological entropy is strictly larger than  $\ln 2$ , which of course contradicts our assumption of binary dynamics. Therefore  $C_0$  is bounded from above by the value 2. This result generalizes to  $k$ -branch symbolic dynamics where  $C_0 \leq k$ . In order to compare the complexities of systems with different alphabets, one should normalize the value of  $C_0$  by the number of alphabet symbols.

#### APPENDIX B

In this appendix, we provide the details leading to the construction of the building blocks in (9) of the quadratic map at parameter value  $a_\infty$ . The preimage relations of the elements of the  $F_{n-1}$  Markov partition elements given in the text [after expression (9)] can be expressed in terms of only those elements possessing two preimages as follows:

$$i \rightarrow \begin{cases} F_{n-3}(1), & F_{n-1}-i(01) \text{ if } i \in [1, F_{n-3}] \\ F_{n-2}(01), & 2F_{n-3}-i(1) \text{ if } i \in [F_{n-3}, 2F_{n-3}] \\ F_{n-2}(01), & i-F_{n-3}(11) \text{ if } i \in [2F_{n-3}, F_{n-1}] \end{cases}$$

where we have relabeled the partition elements by sub-

tracting  $F_{n-2}$  from each of them. Originally, exactly the first  $F_{n-2}$  partition elements had only a single preimage. The symbol codes in parentheses in the above expression denote the symbol sequence of the preimage. For example, the code 01 means that the first preimage of element  $i$  is to the left of the critical point (symbol 0) while its second preimage is to the right of it (symbol 1).

From the above preimage relations, it is clear that each partition element has either partition element  $F_{n-3}$  as its first preimage or else it has partition element  $F_{n-2}$  as its second preimage; all of these preimages are denoted by nonhorizontal lines in Fig. 6. The remaining preimage relations can be represented graphically as the 1D map comprised of three segments  $A$ ,  $B$ , and  $C$  shown in Fig. 11. The traversal sequence of the map can be seen to obey the following rules:

$$B \rightarrow A, \quad C \rightarrow B. \quad (\text{B1})$$

Starting at element  $F_{n-5}$ , which is the right-hand preimage of element  $F_{n-2}$ , and traversing the graph, one obtains an aperiodic sequence of the three branches which ends at partition element  $2F_{n-3}$ . The sequence itself can be constructed using the inflation rule of Eq. (7) with

$$\alpha = AB = 011, \quad \beta = ACB = 01111, \quad (\text{B2})$$

where the last  $\beta$  at the final level of the inflation rule (level  $n-3$ ) is replaced by  $A=01$ . This sequence leads to the labeling of the links on the horizontal line of Fig. 6.

The simplest building block entering element  $F_{n-2}$  is the period-2 cycle labeled 10. The other building blocks entering element  $F_{n-2}$  are obtained by following the link leading to the leftmost node of Fig. 6 and subsequently traversing a segment of the horizontal line to any of the other nodes on the line. At that point, the path turns either downward (if the node is in region A) to node  $F_{n-3}$ , or otherwise (if the node belongs to regions B or C) upwards directly to node  $F_{n-2}$ . The paths that go through node  $F_{n-3}$  return directly to node  $F_{n-2}$  after circling node  $F_{n-3}$  an arbitrary number of times. Note that both

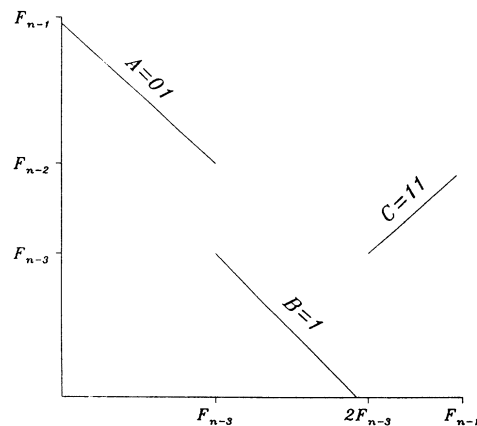


FIG. 11. Preimages of partition elements of the quadratic map at a parameter value approximating  $a = a_\infty$  and possessing a Markov partition with  $F_{n-1}$  elements. Only partition elements lying on the horizontal line of Fig. 6 are shown.

upwards and downwards paths are allowed at the rightmost node on the horizontal of Fig. 6. The building blocks are actually obtained by reading the traversal paths in reverse order since the arrows always point towards preimages. Since the forward iterates of points in

element  $F_{n-2}$  all fall in a single partition element to the left of the critical point, one can express the building blocks in terms of periodic orbits in that particular partition element. The resulting blocks are exactly those in expression (9).

- 
- <sup>1</sup>J.-P. Eckmann and D. Ruelle, *Rev. Mod. Phys.* **57**, 617 (1985).  
<sup>2</sup>P. Grassberger and I. Procaccia, *Phys. Rev. A* **34**, 659 (1984).  
<sup>3</sup>D. Auerbach, P. Cvitanović, J.-P. Eckmann, G. H. Gunaratne, and I. Procaccia, *Phys. Rev. Lett.* **58**, 2387 (1987).  
<sup>4</sup>D. Auerbach, B. O'Shaughnessy, and I. Procaccia, *Phys. Rev. A* **37**, 2234 (1988).  
<sup>5</sup>C. Grebogi, E. Ott, and J. A. Yorke, *Phys. Rev. A* **36**, 3522 (1987); **37**, 1711 (1988).  
<sup>6</sup>G. H. Gunaratne and I. Procaccia, *Phys. Rev. Lett.* **59**, 1377 (1987).  
<sup>7</sup>P. Cvitanović, *Phys. Rev. Lett.* **61**, 2729 (1988).  
<sup>8</sup>A. N. Kolmogorov, *Probl. Inf. Transm. (USSR)* **1**, 1 (1965); G. Chaitin, *J. Assoc. Comput. Mach.* **13**, 547 (1966).  
<sup>9</sup>A. Lempel and J. Ziv, *IEEE Trans. Inf. Theory* **22**, 75 (1976).  
<sup>10</sup>J. E. Hopcroft and J. D. Ullman, *Introduction to Automata Theory, Language and Computation* (Addison-Wesley, Reading, MA, 1979).  
<sup>11</sup>S. Wolfram, *Commun. Math. Phys.* **96**, 15 (1984).  
<sup>12</sup>P. Grassberger, *Int. J. Theor. Phys.* **25**, 939 (1986).  
<sup>13</sup>J. Crutchfield and K. Young, *Phys. Rev. Lett.* **63**, 109 (1989).  
<sup>14</sup>J.-P. Eckmann and I. Procaccia, *Phys. Rev. A* **34**, 659 (1986).  
<sup>15</sup>I. Procaccia, S. Thomae, and C. Tresser, *Phys. Rev. A* **35**, 1884 (1987).  
<sup>16</sup>J. Hartmanis, *Proceedings of the 24th IEEE Symposium on the Foundations of Computer Science* (Institute of Electrical and Electronic Engineers, New York, 1983), p. 439; M. Sipser, *Proceedings of the 15th Association for Computer Machinery Symposium on the Theory of Computing* (Association for Computer Machinery, New York, 1983), p. 330.  
<sup>17</sup>C. H. Bennett, *Found. Phys.* **16**, 585 (1986).  
<sup>18</sup>P. Collet and J.-P. Eckmann, *Iterated Maps on the Interval as Dynamical Systems* (Birkhauser, Boston, 1980).  
<sup>19</sup>C. Grebogi, E. Ott, and J. A. Yorke, *Phys. Rev. Lett.* **48**, 1507 (1982).  
<sup>20</sup>A. Rényi, *Proceedings of the Fourth Berkeley Symposium on Mathematical Statistics and Probability* (University of California Press, Berkeley, 1961), p. 547.  
<sup>21</sup>D. Ruelle; *Thermodynamic Formalism* (Addison-Wesley, Reading, MA, 1978); R. Bowen, *Lect. Notes Math.* **470**, 1 (1975); Y. Sinai, *Russ. Math. Surv.* **166**, 21 (1972).  
<sup>22</sup>T. Bohr and D. Rand, *Physica* **25**, 387 (1987).  
<sup>23</sup>D. Katzen and I. Procaccia, *Phys. Rev. Lett.* **58**, 1169 (1987).  
<sup>24</sup>P. Szépfalussy and G. Györgyi, *Phys. Rev. A* **33**, 2852 (1986).  
<sup>25</sup>A. Csordás and P. Szépfalussy, *Phys. Rev. A* **38**, 2582 (1988).  
<sup>26</sup>S. Grossman and S. Thomae, *Z. Naturforsch. A* **32**, 1353 (1977).  
<sup>27</sup>M. Hénon, *Commun. Math. Phys.* **50**, 69 (1976).  
<sup>28</sup>P. Grassberger and H. Kantz, *Phys. Lett.* **113A**, 235 (1985).  
<sup>29</sup>P. Cvitanović, G. H. Gunaratne, and I. Procaccia, *Phys. Rev. A* **38**, 1503 (1988).  
<sup>30</sup>D. Auerbach (unpublished).  
<sup>31</sup>L. P. Hurd, *Complex Syst.* **1**, 69 (1987).